



Influence of different bacterial strains on cracks self-healing in cement-based matrices with and without incorporated air

Sheila Karine Lenz¹ · Edna Possan¹ · Michel Rodrigo Zambrano Passarini² · Polyana Ghellere¹

Received: 24 April 2023 / Revised: 17 May 2023 / Accepted: 18 May 2023 / Published online: 1 June 2023
© The Author(s), under exclusive licence to Springer Nature Switzerland AG 2023

Abstract

Biological self-healing occurs by metabolically calcium carbonate (CaCO_3) precipitating bacteria. However, the cementitious matrix is hostile, and it is necessary to create a favorable environment for the prolonged viability of the bacteria. In this context, this study aimed to evaluate the efficiency of three bacterial strains in the self-healing of cracks (*Bacillus subtilis*—AP91, *Bacillus cf. subtilis*—BS, and *Bacillus cf. cereus*—BC) incorporated into the mixing water of cementitious mortars with and without air admixture. After 1 and 7 days of curing, realistic cracks were induced in the $40 \times 40 \times 160$ mm prismatic specimens' central region. Compressive strength and flexural tensile strength tests and image analysis in optical stereomicroscope and SEM were performed at different control ages for specimens in wet curing. It was verified that the bacterial strain influences the self-healing performance, with better results for BS, with healing rates of 95.72% in cracks with a thickness of 1.58 mm. Incorporating air into the mixture proved favorable to self-healing, with rates up to 126% higher than the same variation without the additive. The studied process is a promising biotechnological solution for recovering micro-cracks in cement-based materials, potentially increasing the matrix's durability and strength.

Keywords *Bacillus* · Self-healing concrete · Biological self-healing · Air-incorporating additive

1 Introduction

Cracks are common pathological manifestations in concrete structures, which may compromise durability as they allow liquids, gases, and other aggressive agents to enter into the matrix, exposing the concrete reinforcement to corrosion and increasing the risk of the constructions' partial or total collapse [1–3]. Aiming to minimize the problems associated

with cracks to make concrete more durable and sustainable, the search for new technologies, such as the self-healing of cementitious materials [4–7], is on the rise. This self-healing naturally occurs mainly in two ways: with the cement's anhydrous portions in the matrix; or, in a more considerable way, when the calcium ions (Ca^{2+}) present in the cementitious material's water pores react with the carbonate ions (CO_3^{2-}) found in the crack water forming calcium carbonate (CaCO_3) [8]. Therefore, exploring CaCO_3 intentional precipitation in cement-based matrices may be highly advantageous for the crack recovery process [3], which may be carried out by bacteria.

Crack repair by a healing agent easily found in nature integrated into the cementitious material, such as bacteria, may be a promising biotechnological tool for maintaining structures, especially in places with difficult access or requiring interruption of activities for repair [3, 9]. Using bacteria that precipitate CaCO_3 biologically in cementitious materials may close cracks, decrease voids, and inherently reduce porosity, increase compressive strength and service life of concretes and mortars [4, 5, 10].

The diversity of existing bacteria is vast, but not all are suitable for incorporation into cement-based materials. The

✉ Edna Possan
epossan@gmail.com

Sheila Karine Lenz
sheila_lenz@icloud.com

Michel Rodrigo Zambrano Passarini
michel.passarini@unila.edu.br

Polyana Ghellere
p_ghellere@hotmail.com

¹ Latin American Institute of Technology, Infrastructure and Territory, Federal University of Latin American Integration, UNILA, Foz do Iguaçu, Brazil

² Latin American Institute of Life and Nature Sciences, Federal University of Latin American Integration, UNILA, Foz do Iguaçu, Brazil

bacteria must first pose no risk to people's health or the environment for this use. Moreover, they must be alkali resistant and able to form spores—extremely resistant biological structures—to ensure survival in highly alkaline environments such as concrete, without nutrients and with oxygen only in the pores and surface [9, 11]. If incorporated into the matrix along with the mixing water, they must be resistant to the mechanical mixing of the cementitious material [9].

Bacteria of the genus *Bacillus* have been highlighted in the literature for this use [9]. However, even with appropriate bacteria, the continuous decrease in pore diameter over the lifetime of concrete and mortar may crush bacterial spores, compromising their durability in cementitious materials. Micro-pores are created in the matrix by incorporating air into the mixture, enabling the survival of bacteria [12]. However, air incorporation that seems favorable to the bacterial action usually reduces the mechanical properties of the matrix, which is not desirable from the point of view of mechanical performance. Therefore, studies are needed to evaluate the efficacy of adding air to bacterial self-healing in cement-based materials without impairing the material's mechanical properties. Furthermore, the same strain of microorganisms may present different performances in calcium carbonate precipitation. It is essential to find strains with higher precipitation potential, in line with the aim of this study.

The study scenarios are vast, and this study aims to contribute to a better understanding of the self-healing process utilizing CaCO_3 precipitating biological agents, evaluating the self-healing of cracks performed by three bacterial strains, *Bacillus subtilis* (AP91), *Bacillus cf. subtilis* (BS) and *Bacillus cf. cereus* (BC), into matrices with and without incorporated air. The study contributes to developing biomaterials for crack recovery in Portland cement-based materials to reduce environmental impacts, consumption of natural resources, and costs associated with the materials used in civil construction, contributing to durability, service life, and sustainability of the built environment.

2 Materials and methods

2.1 Microorganisms preparation

The used bacteria (Table 1) were isolated by Ghellere [13], preserved in glycerol in cryotubes at $-20\text{ }^\circ\text{C}$ and reactivated using the NA medium seeding technique, and then stored in an oven at $37\text{ }^\circ\text{C}$ for 24 to 48 h (Fig. 1).

The three strains' bacterial culture was performed in Mueller Hinton (MH) liquid culture medium as it presents a higher concentration of spores per mL [14]. The flasks containing the medium and the biological agents were shaken for 66 h using a shaker at 130 rpm and an average

Table 1 Species, nomenclature, and bacteria used in the study

Nomenclature	Identification	Origin
AP91	<i>Bacillus subtilis</i> AP91	Rice husk (Embrapa)
BS	<i>Bacillus cf. subtilis</i>	Building wall in Foz do Iguaçu (Brazil)
BC	<i>Bacillus cf. cereus</i>	Itaipu Dam

temperature of $37\text{ }^\circ\text{C}$ to favor bacterial growth, according to [13].

For a higher concentration of bacteria, the solution was washed to remove the culture medium by agitation in a centrifuge at 3600 rpm for 20 min, replacing the supernatant medium with 0.85% NaCl saline solution. The washing process was performed twice as per the methodology in the literature [14]. Then the bacteria were induced to spore formation, keeping the solution with the microorganisms at rest for 2 days in a refrigerator at $8\text{ }^\circ\text{C}$ [14].

The sporulated bacteria were quantified with the optical density (OD) test in a spectrophotometer, using 2 mL of each bacterial solution. 2 mL of 0.85% NaCl saline solution was used as a reference. The optical density reading of each solution was performed in duplicate at 600 nm wavelength. Bacteria concentration was calculated using Eq. 1 [15] for each solution.

$$Y = 8,59 * 10^7 * X^{1,3627} \quad (1)$$

where: Y = Bacterial concentration in spores per ml.
X = Optical density or absorbance reading.

Based on the bacterial concentration found, dilution calculations were performed to obtain the required concentration (106 spores/mL). After quantification, the spores in suspension were stored in a refrigerator until applying them in the cementitious materials [9].

2.2 Mortar production

The mortars were produced using Portland cement of high initial strength (CP V-ARI—equivalent to CEM I of ASTM C 150) with $\gamma = 3.11\text{ g/cm}^3$, D50 $14.8\text{ }\mu\text{m}$, and blaine of $5320\text{ cm}^2/\text{g}$, natural sand of quartz origin ($\gamma = 5.51\text{ g/cm}^3$) and air-entraining additive, physically and chemically characterized according to current standards. Eight variations of cement-based mortar were produced (1:3:0.48 ratio, cement, sand, and water), varying the three bacterial strains (AP91, BC, and BS) and the presence or absence of air admixture (0.05% content) (Table 2).

Due to the difficulty of opening realistic cracks, prismatic specimens ($40 \times 40 \times 4460\text{ mm}$) were produced, following NBR 13279 standard, with and without reinforcement. For the group of specimens with reinforcement, cylindrical

Fig. 1 Bacteria visible in the depletion streaks on Petri dishes



Table 2 Mortars produced’s composition and nomenclature

Nomenclature (reinforced)	Nomenclature (unreinforced)	Bacteria	AIR (%)
M-REF	M-REF-A	–	–
AP91	AP91-A	<i>Bacillus subtilis</i> AP91	
BS	BS-A	<i>Bacillus cf. subtilis</i>	
BC	BC-A	<i>Bacillus cf. cereus</i>	
M-REFair	M-REFair-A	–	0.05%
AP91air	AP91air-A	AP91	0.05%
BSair	BSair-A	BS	0.05%
BCair	BCair-A	BC	0.05%

spacers of cement paste were molded in the mortar’s ratio of the study (1:0.48—cement: water), with ribs for the reinforcement fitting inserted in the mold at approximately 1.0 cm from the base.

The mortars were produced in a mechanical stirrer, diluting the bacterial solution in water according to the desired concentration (106 spores/mL) and deducting the volume of solution used from the mixing water. The specimens were cured-submerged in water for crystals’ greater precipitation [16, 17]. For this, they were placed in containers with water open to the atmosphere to allow oxygen and carbon dioxide to enter [18]. They were separated by bacteria keeping the specimens always in the same position, with the cracked sides facing upwards. When the specimens were removed

from the submerged curing (for visual inspection and tests) and returned to the container, the curing water was changed to simulate natural water renewal conditions.

2.3 Crack opening and visual analysis

A manual cracking protocol was defined for crack opening with a bench vice and 4 supports (Fig. 2a) since the mortars presented low tensile strength with a fragile rupture. In this process, it was not possible to establish the cracking load nor to control the crack opening size, which presented thicknesses ranging from (Fig. 2b) 0.38 to 2.84 mm (Table 5).

48 specimens (24 with and 24 without reinforcement—in triplicate per variable) were visually analyzed using an optical stereomicroscope Zeiss Discovery. V12, with Zeiss PlanApo S 1.0×FWD 60 mm lens, connected to a Zeiss Axiocam 105 camera with up to 100× magnification, and with AxioVision SE64 software to evaluate the self-healing of mortar specimens by the closing of cracks over time. The unreinforced specimens were photographed at ages 1 (reading 0), 14, 21, 28, 42, and 56 days, and the reinforced specimens at ages 7 (reading 0), 14, 21, 28, 42, 56, and 70. For visualization and reading in the Stereomicroscope, all specimens’ cracks were marked and divided into 8 approximately equidistant zones (Fig. 3), adapting the reading procedure from the literature [19] and generating 2496 images.

A healed area selection and calculation method, aiming to quantify the self-healing evolution along the time for all

Fig. 2 Opening of cracks in prismatic specimens by means of manual loading in a 4-point bench vice a protocol used b resulting cracks



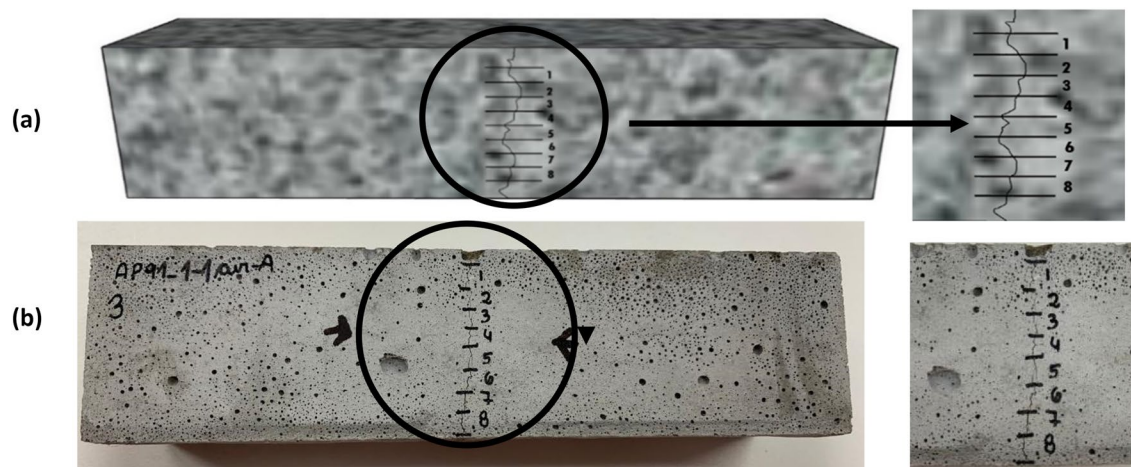


Fig. 3 Division of the cracks into 8 spaces for visualization with an optical microscope **a** schematic and **b** real photos

mortars, was developed and shown in Table 3. Steps 1, 2, 3, and 4 aimed at reducing the number of images, making it possible to calculate the area of the crack. Step 5 was employed because, in some situations, it was noticed the closing was only superficial or only of the bottom of the crack. However, as there was carbonate precipitation, it was not possible to disregard it. It was noticed in Step 7 that the cracks' healing rate (t_c) among distinct specimens was similar; however, the thickness of the cracks differed.

As smaller cracks are likely to close more easily and in less time [13], it was necessary to differentiate healing by associating them with the average thickness (T_m) of each crack, thus creating the index of self-healing (I_C). The calculations used to obtain the healing index are in Eq. 2.

$$I_C = \left(\frac{A_0 - A_{age}}{A_0} \right) \times T_m \times 100 \quad (2)$$

where: I_C = Index of self-healing cracks (%). A_0 = Initial crack area measurement (mm^2). A_{age} = Crack area

measurement at reading age (mm^2). T_m = Initial crack average thickness (mm).

A sample fragment from the crack region was analyzed by scanning electron microscopy (SEM) to observe the precipitated crystals' morphology. The fragment was obtained by pre-cutting with a micro grinder near the crack wall. Then the desired fragment was removed and positioned on the stubs using a metal wedge and a hammer. After surface deposition of palladium gold film, the specimens were analyzed in a ZEISS EVO MA10 Scanning Electron Microscope, operating at 20 kV voltage and running SmartSEM software, with Energy Dispersive Spectroscopy (EDS).

2.4 Evaluation of flexural tensile and compressive strength

Three-point flexural tensile and axial compressive strength tests were performed on all mortar variations at 28 and 56 days of submerged curing on intact specimens (Table 4). For each mix, specimens were produced in triplicate, with dimensions of $40 \times 40 \times 160$ mm [20].

Table 3 Specimens' self-healing calculation methodology over time

Stage	Procedure
1	Selection of the best self-healing sample, among three of each trace, according to the dynamic modulus of elasticity recovery result determined by the impulse excitation technique (IET)
2	Discard the crack edge sections
3	3 largest crack's visual selection from the selected specimen
4	Images delineation at ages 7, 14, 28, and 70 days on the reinforced specimens and 1, 14, 28, and 56 days on the unreinforced specimens
5	Crack area calculation at each age (when the closure is only superficial or only at the bottom, the area was divided by 2)
6	Crack self-healing rate calculation by age
7	Specimens self-healing index calculation by multiplying the self-healing rate x average crack thickness

3 Results and discussions

3.1 Reinforced cracks specimens self-healing

Table 5 shows the reinforced specimens' self-healing results with and without incorporated air, varying the biological agents under study. It was noted that all the specimens, including those without added bacteria (reference), presented precipitation of carbonate crystals, with the cracks closure in a punctual or continuous way. The precipitated products presented whitish coloration and branched shape, corroborating the literature [8]. The precipitation and coloration under these conditions were attributed to the calcite form [21].

Specimens' self-healing reached 100% rates for the without-AIR specimens with a 0.46 mm average thickness and 0.57 mm maximum thickness. For the air-incorporated specimens, cracks with a 0.37 mm average thickness and a 0.40 mm maximum opening healed 100%. Such closure is autogenous self-healing, verified in other studies [17, 19, 22]. Under similar curing conditions, continuous healing was observed in cracks with a 0.55 mm thickness and punctual healing up to 0.60 mm [17]. The specimens added with BS agent also presented a 100% healing rate in cracks with a 0.58 mm maximum thickness. The specimens added with AP91 and BSair bacteria presented a 99.65% and 98.79% healing rate for cracks with a 0.55 and 0.82 mm maximum thickness, respectively.

In some situations, as in the specimens containing AP91, the continuous crack closing occurred in some zones in the first 7 days of opening [23]. Reported that the CaCO_3 formation reaction by the bacteria's metabolic activity occurs quickly, as also verified in this study. However, the situation was not verified in all zones with the same variation, demonstrating no healing time linearity, even in specimens with the same composition.

Specimens with and without biological agents presented self-healing, indicating combined autogenous and autonomous processes. Specimens with bacteria presented superior performance to the reference specimens, with the cracks closing with larger openings, confirming the potential of using bacteria for crack recovery.

In the reference specimens, healing product formation may be due to the cement secondary hydration since the cracking was performed at 7 days, with anhydrous material still in the matrix [24]. Compositions with low w/c ratios may be favorable for autogenous self-curing since even after some curing time has passed, significant amounts of unhydrated binder may remain, which are potentially available for delayed hydration reaction and carbonation [25]. There may also be the CaCO_3 formation by a reaction between the calcium in the matrix and the carbonate ions supplied by the curing water [26].

It was verified for BCair specimens fewer healing products in the crack region at 21 and 28 days than at 14 days. The same occurred in BSair specimens' crack area, as shown in Fig. 4, where at 14 days, precipitated product crystals on the crack edge occurred, not visible at the subsequent reading ages (21 and 28 days). For advanced analysis ages (42 and 70 days), total crack closure was observed.

According to [17], a detachment occurs due to the dropping or rupture of the product generated on the crack wall, resulting from handling the specimen or the leaching process. After non-destructive control tests, the specimens re-submersion may generate water pressure on the healing products, causing its detachment and consequent dropping in the region. The study by Roig-Flores et al. [27] suggested that no intermediate measurements should be performed to avoid the accidental removal of newly formed precipitates (7, 14, and 21 days), as they may affect the self-healing performance. If intermediate readings are carried out, a follow-up of the specimens' leaching process by measuring pH and conductivity to check their influence on the process is essential.

Table 4 Characteristics and number of specimens, testing age, and standard used

Test	Condition of specimens	N° of specimens	Dimension (mm)	Test age (days)	Standard
Realistic cracking of specimens	Reinforced	24	40×40×160	7	–
	Unreinforced	24	40×40×160	1	–
Flexural tensile strength	Unreinforced/entire	48	40×40×160	28 and 56	NBR 13279 (ABNT, 2005)
Compressive strength	Unreinforced/entire	96 ¹	≅40×40×80	28 e 56	
Visual inspection of cracks in optical stereomicroscope	Reinforced	24	40×40×160	7, 14, 21, 28, 42, 56 e 70	–
	Unreinforced	24	40×40×160	1, 14, 21, 28, 42 e 56	–
Visual inspection of cracks in SEM	Reinforced	3	≅5×5×2	77	–
	Unreinforced	1	≅5×5×2	77	–

¹Compressive strength specimens from complete damage in the flexural tensile strength test

Table 5 Self-healing in cracked areas over time for reinforced specimens





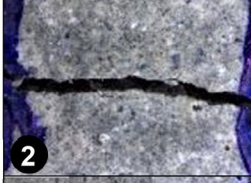
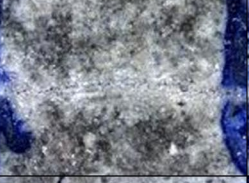



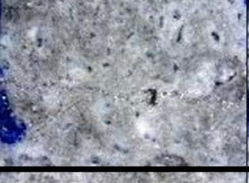
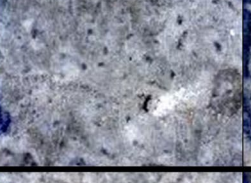
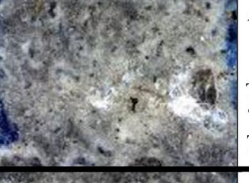

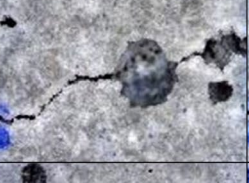




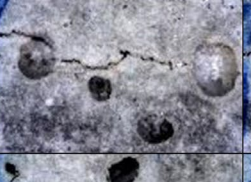
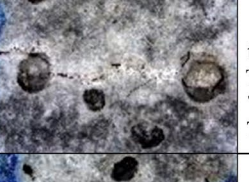

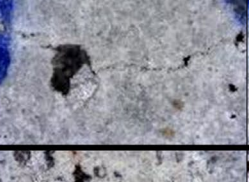





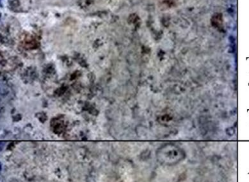



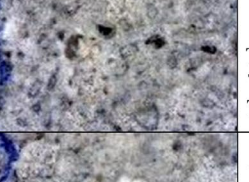




	7 DAYS (L ₀)	14 DAYS	28 DAYS	70 DAYS	SUMMARY
AP91					$A_0 = 2.50 \text{ mm}^2$ $t_m = 0.43 \text{ mm}$ $t_{max} = 0.50 \text{ mm}$ $T_{C14} = 72.80\%$ $T_{C28} = 80.80\%$ $T_{C70} = 87.60\%$
					$A_0 = 4.28 \text{ mm}^2$ $t_m = 0.55 \text{ mm}$ $t_{max} = 0.55 \text{ mm}$ $T_{C14} = 87.15\%$ $T_{C28} = 95.80\%$ $T_{C70} = 99.65\%$
					$A_0 = 5.66 \text{ mm}^2$ $t_m = 0.72 \text{ mm}$ $t_{max} = 2.15 \text{ mm}$ $T_{C14} = 55.83\%$ $T_{C28} = 56.89\%$ $T_{C70} = 88.16\%$
AP91air					$A_0 = 9.55 \text{ mm}^2$ $t_m = 1.2 \text{ mm}$ $t_{max} = 2.84 \text{ mm}$ $T_{C14} = 20.74\%$ $T_{C28} = 23.98\%$ $T_{C70} = 72.04\%$
					$A_0 = 1.61 \text{ mm}^2$ $t_m = 0.37 \text{ mm}$ $t_{max} = 0.50 \text{ mm}$ $T_{C14} = 65.22\%$ $T_{C28} = 72.05\%$ $T_{C70} = 86.96\%$
					$A_0 = 4.03 \text{ mm}^2$ $t_m = 0.74 \text{ mm}$ $t_{max} = 2.09 \text{ mm}$ $T_{C14} = 20.84\%$ $T_{C28} = 36.23\%$ $T_{C70} = 72.95\%$
BC					$A_0 = 2.36 \text{ mm}^2$ $t_m = 0.57 \text{ mm}$ $t_{max} = 0.6 \text{ mm}$ $T_{C14} = 28.81\%$ $T_{C28} = 41.53\%$ $T_{C70} = 94.92\%$
					$A_0 = 3.48 \text{ mm}^2$ $t_m = 0.55 \text{ mm}$ $t_{max} = 0.92$ $T_{C14} = 10.63\%$ $T_{C28} = 19.83\%$ $T_{C70} = 65.52\%$
					$A_0 = 3.82 \text{ mm}^2$ $t_m = 0.41 \text{ mm}$ $t_{max} = 0.44 \text{ mm}$ $T_{C14} = 11.52\%$ $T_{C28} = -1.83\%$ $T_{C70} = 76.57\%$

Table 5 (continued)


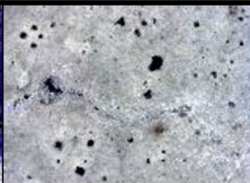
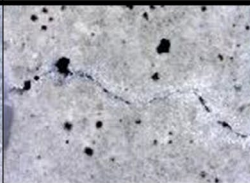







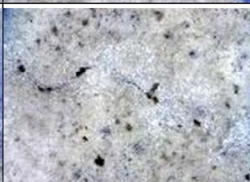
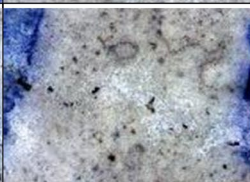
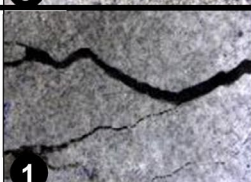
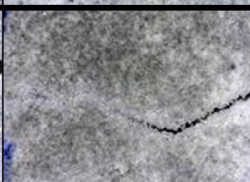
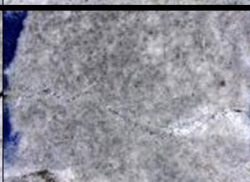




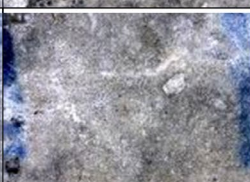

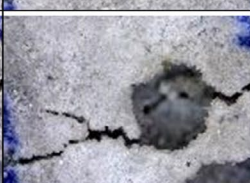

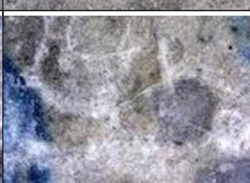

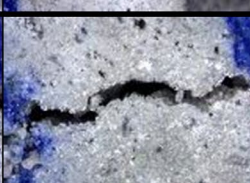
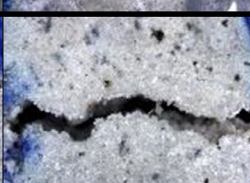
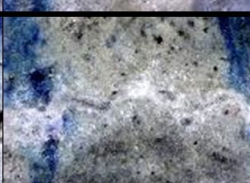

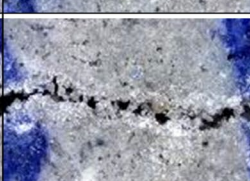
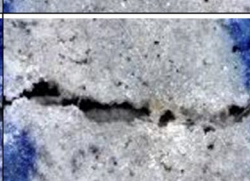
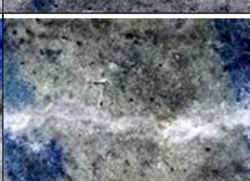

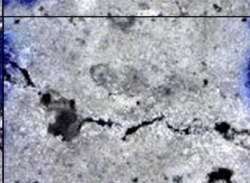
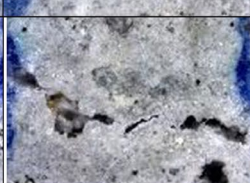
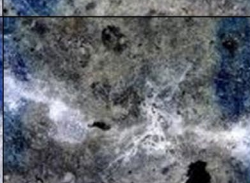
	7 DAYS (L ₀)	14 DAYS	28 DAYS	70 DAYS	SUMMARY
BCair					$A_0 = 3.25\text{mm}^2$ $t_m = 0.36\text{mm}$ $t_{max} = 0.39\text{mm}$ $T_{C14} = 55.38\%$ $T_{C28} = 72.31\%$ $T_{C70} = 86.46\%$
					$A_0 = 4.51\text{mm}^2$ $t_m = 0.65\text{mm}$ $t_{max} = 1.03$ $T_{C14} = 75.61\%$ $T_{C28} = 65.41\%$ $T_{C70} = 77.61\%$
					$A_0 = 4.02\text{mm}^2$ $t_m = 0.54\text{mm}$ $t_{max} = 0.84\text{mm}$ $T_{C14} = 85.32\%$ $T_{C28} = 79.35\%$ $T_{C70} = 91.04\%$
BS					$A_0 = 4.81\text{mm}^2$ $t_m = 0.53\text{mm}$ $t_{max} = 0.58\text{mm}$ $T_{C14} = 79.21\%$ $T_{C28} = 90.65\%$ $T_{C70} = 100\%$
					$A_0 = 4.98\text{mm}^2$ $t_m = 0.5\text{mm}$ $t_{max} = 0.55\text{mm}$ $T_{C14} = 57.23\%$ $T_{C28} = 88.96\%$ $T_{C70} = 95.38\%$
					$A_0 = 4.00\text{mm}^2$ $t_m = 0.65\text{mm}$ $t_{max} = 1.03\text{mm}$ $T_{C14} = 48.00\%$ $T_{C28} = 83.25\%$ $T_{C70} = 96.25\%$
BSair					$A_0 = 6.3\text{mm}^2$ $t_m = 0.85\text{mm}$ $t_{max} = 0.9\text{mm}$ $T_{C14} = 35.56\%$ $T_{C28} = 13.65\%$ $T_{C70} = 91.43\%$
					$A_0 = 5.39\text{mm}^2$ $t_m = 0.78\text{mm}$ $t_{max} = 0.82\text{mm}$ $T_{C14} = 63.45\%$ $T_{C28} = 21.15\%$ $T_{C70} = 98.79\%$
					$A_0 = 6.77\text{mm}^2$ $t_m = 0.91\text{mm}$ $t_{max} = 1.58\text{mm}$ $T_{C14} = 59.08\%$ $T_{C28} = 56.13\%$ $T_{C70} = 95.72\%$

Table 5 (continued)

	7 DAYS (L ₀)	14 DAYS	28 DAYS	70 DAYS	SUMMARY
M-REF					$A_0 = 4.26\text{mm}^2$ $t_m = 0.50\text{mm}$ $t_{max} = 0.53\text{mm}$ $TC_{14} = 74.90\%$ $TC_{28} = 79.34\%$ $TC_{70} = 93.90\%$
					$A_0 = 12.23\text{mm}^2$ $t_m = 0.83\text{mm}$ $t_{max} = 1.54\text{mm}$ $TC_{14} = 79.56\%$ $TC_{28} = 63.04\%$ $TC_{70} = 58.71\%$
					$A_0 = 2.31\text{mm}^2$ $t_m = 0.46\text{mm}$ $t_{max} = 0.57\text{mm}$ $TC_{14} = 90.91\%$ $TC_{28} = 80.52\%$ $TC_{70} = 100\%$
M-REFair					$A_0 = 2.72\text{mm}^2$ $t_m = 0.35\text{mm}$ $t_{max} = 0.38\text{mm}$ $TC_{14} = -20.0\%$ $TC_{28} = 44.12\%$ $TC_{70} = 88.24\%$
					$A_0 = 3.45\text{mm}^2$ $t_m = 0.37\text{mm}$ $t_{max} = 0.40\text{mm}$ $TC_{14} = 13.62\%$ $TC_{28} = 86.96\%$ $TC_{70} = 100\%$
					$A_0 = 2.55\text{mm}^2$ $t_m = 0.29\text{mm}$ $t_{max} = 0.33\text{mm}$ $TC_{14} = 65.10\%$ $TC_{28} = 92.55\%$ $TC_{70} = 94.51\%$

Analysis of 3 cracked areas from each group, where: A_0 : Initial crack area on the day of cracking; t_m : average crack thickness; t_{max} : the maximum thickness of each crack, Rh_x = Healing rate by age

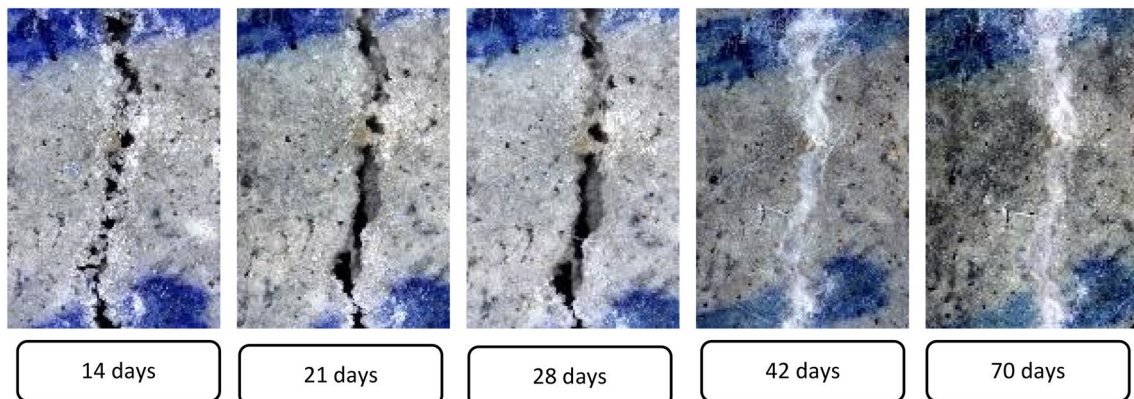


Fig. 4 Precipitated product detachment at the crack edge on BSair specimens

No proportionality between average crack thickness and healing rate was noticed since the closing area is not bigger in smaller crack thicknesses [13]. Observed greater success in cracks self-healing with openings smaller than 0.43 mm (for non-submerged specimens). Similar results to the present study were noticed by [22], who obtained higher and faster autogenous healing rates in larger cracks in air-conditioned mortar specimens [22]. Reported that the self-healing product precipitation kinetics is greater in cracks of greater thickness since there is no space limitation for product formation with enough openings for external CO_2 and water supply for CaCO_3 formation.

By analyzing the healing index (healing rate multiplied by the average crack thickness), it was observed (Fig. 5) that all combinations improved over time, with more favorable results for AIR-incorporated matrices, except in those without bacteria (reference).

The reference specimen presented the highest healing index at 14 days (7 days after the crack opening), indicating that autonomous self-healing occurred primarily at early ages due to hydration product formation in the matrix. For 28 and 70 days, higher healing indexes for specimens with bacteria addition were observed, indicating that the microorganisms may be acting and favoring the cracks' autonomous self-healing in the last ages.

The lower healing index at 28 days for some specimens was associated with the precipitated product's detachment. In the first healing ages, the compounds formed did not adhere well to the crack walls and could be easily removed by the leaching process or action resulting from handling the submerged specimens.

The best results were obtained for the BSair, AP91air, and BS specimens, which presented healing indexes of 80.63%, 57.54%, and 54.42%, respectively. It must be highlighted that these mortars have the *Bacillus subtilis* species bacteria. This strain has already been used in other studies [13, 14, 17, 28], presenting satisfactory self-healing results.

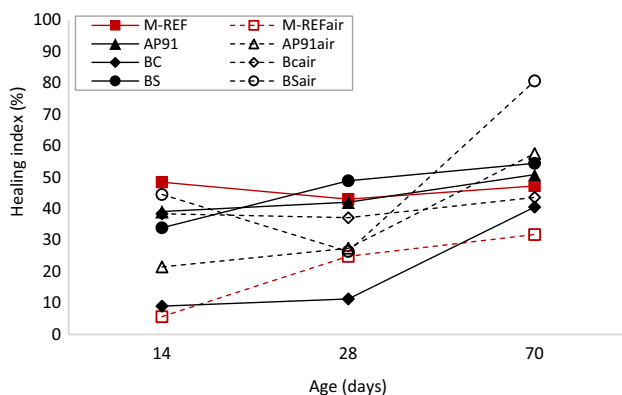


Fig. 5 Healing index over time in cracked and reinforced specimens

3.2 Cracks self-healing in non-reinforced specimens

Table 6 presents the images and data of the cracked zones over time for unreinforced cracked specimens. It was observed that no cracked zone showed 100% self-healing. The best results obtained in this group were for AP91air specimens, with a 92.29% healing rate at 56 days in the cracked zone with $t_{\max} = 1.62$ mm, BCair specimens with 99.17% healing rate in the cracked zone with $t_{\max} = 0.53$ mm and for the BS specimens with 94.09% healing rate at $t_{\max} = 0.73$ mm, which also presented closing of a pore present in the cracked face.

The images in Table 6 showed a reduction in the healing rate for some specimens (M-REFair, M-REF, BSair, BC, BCair), similar to that in the reinforced specimens, due to the probable precipitated products' detachment. Figure 6 shows the healing index of specimens over time.

A high healing index was observed for AP91air specimens. All specimens containing bacteria presented Rh results higher than the M-REF specimens, demonstrating the efficacy of using biological agents in self-healing cracks in cementitious materials, corroborating with studies of [9, 13, 17, 18, 28]. Furthermore, a higher healing index was noticed for air-incorporated specimens, in agreement with studies of [29, 30], except for the BSair variation.

A more effective self-healing process was noted for reinforced specimens when comparing the final healing index between reinforced (70 days) and unreinforced (56 days) specimens (Fig. 7). For the unreinforced specimens, the crack closing occurred only punctually in some mixtures, including the reference specimens, without air incorporation. It may be associated with the cohesive nature intrinsic to cracks in cementitious materials, which may be intensified by reinforcement [25].

The visual analysis showed that the cracks' thickness varied with the specimens, hampering the comparative analysis of specimens as reported in the literature [13, 17]. The healing index was suggested, which considers the dimension of the specimens' initial crack opening. This variation is mainly due to the difficulty of opening cracks in nearly fragile materials such as cement-based materials. To minimize this variation [17], recommended that actions be taken to restrict deformation in the matrix and obtain standard thickness cracks. The literature [31] also suggested that when a method for openings standardization is non-existent, the cracking of many specimens should be performed for a later selection of cracks with similar thicknesses for the study groups.

The use of reinforcement facilitates the opening of cracks in the specimens; however, they affect the results of non-destructive tests, such as the ultrasonic wave propagation speed and the modulus of elasticity measurement by the impulse excitation technique (IET), among

Table 6 Analysis of cracked zones' self-healing of unreinforced specimens over time




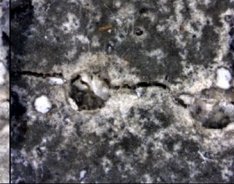




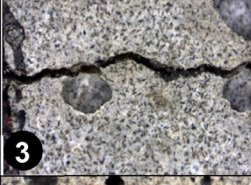

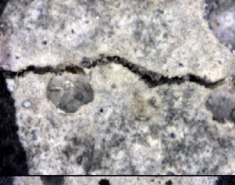
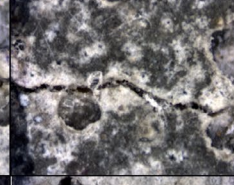
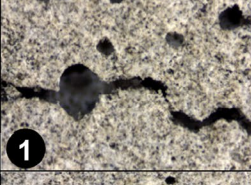
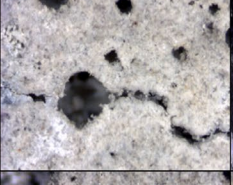

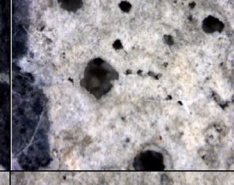
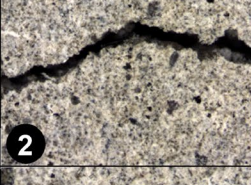



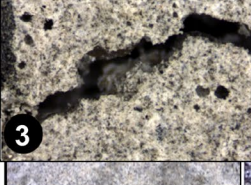

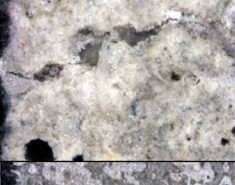
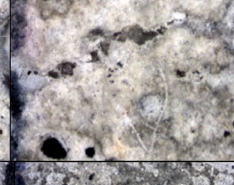




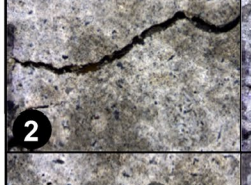





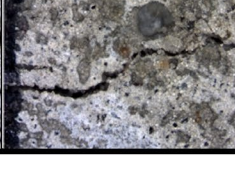

	7 DAYS (L ₀)	14 DAYS	28 DAYS	56 DAYS	SUMMARY
AP91					$A_0 = 4.25 \text{ mm}^2$ $t_m = 0.77\text{mm}$ $t_{max} = 1.80\text{mm}$ $T_{C14} = 14.59\%$ $T_{C28} = 10.12\%$ $T_{C56} = 48.47\%$
					$A_0 = 2.46 \text{ mm}^2$ $t_m = 0.36 \text{ mm}$ $t_{max} = 0.38\text{mm}$ $T_{C14} = 15.85\%$ $T_{C28} = 34.55\%$ $T_{C56} = 63.01\%$
					$A_0 = 3.15 \text{ mm}^2$ $t_m = 0.38\text{mm}$ $t_{max} = 0.57\text{mm}$ $T_{C14} = 18.73\%$ $T_{C28} = 36.19\%$ $T_{C56} = 74.92\%$
AP91air					$A_0 = 3.52 \text{ mm}^2$ $t_m = 0.48\text{mm}$ $t_{max} = 0.52\text{mm}$ $T_{C14} = 62.50\%$ $T_{C28} = 76.70\%$ $T_{C56} = 92.90\%$
					$A_0 = 6.61 \text{ mm}^2$ $t_m = 0.75\text{mm}$ $t_{max} = 1.24\text{mm}$ $T_{C14} = 76.70\%$ $T_{C28} = 85.02\%$ $T_{C56} = 91.83\%$
					$A_0 = 9.86\text{mm}^2$ $t_m = 0.99\text{mm}$ $t_{max} = 1.62\text{mm}$ $T_{C14} = 72.01\%$ $T_{C28} = 90.67\%$ $T_{C56} = 92.29\%$
BC					$A_0 = 3.91 \text{ mm}^2$ $t_m = 0.42\text{mm}$ $t_{max} = 0.96\text{mm}$ $T_{C14} = 44.76\%$ $T_{C28} = 61.64\%$ $T_{C56} = 59.08\%$
					$A_0 = 2.83 \text{ mm}^2$ $t_m = 0.29\text{mm}$ $t_{max} = 0.31\text{mm}$ $T_{C14} = 29.68\%$ $T_{C28} = 56.54\%$ $T_{C56} = 53.71\%$
					$A_0 = 3.14 \text{ mm}^2$ $t_m = 0.29\text{mm}$ $t_{max} = 0.44\text{mm}$ $T_{C14} = 33.44\%$ $T_{C28} = 50.64\%$ $T_{C56} = 39.17\%$

Table 6 (continued)

	7 DAYS (L ₀)	14 DAYS	28 DAYS	56 DAYS	SUMMARY
<i>BCair</i>					$A_0 = 2.42 \text{ mm}^2$ $t_m = 0.32\text{mm}$ $t_{max} = 0.53\text{mm}$ $TC_{14} = 72.73\%$ $TC_{28} = 70.66\%$ $TC_{56} = 99.17\%$
					$A_0 = 2.31 \text{ mm}^2$ $t_m = 0.30\text{mm}$ $t_{max} = 0.33\text{mm}$ $TC_{14} = 43.29\%$ $TC_{28} = 52.38\%$ $TC_{56} = 96.97\%$
					$A_0 = 4.96 \text{ mm}^2$ $t_m = 0.65\text{mm}$ $t_{max} = 1.56\text{mm}$ $TC_{14} = 60.69\%$ $TC_{28} = 61.29\%$ $TC_{56} = 83.47\%$
<i>BS</i>					$A_0 = 5.86 \text{ mm}^2$ $t_m = 0.64\text{mm}$ $t_{max} = 0.72\text{mm}$ $TC_{14} = 39.59\%$ $TC_{28} = 45.90\%$ $TC_{56} = 61.43\%$
					$A_0 = 5.08\text{mm}^2$ $t_m = 0.59\text{mm}$ $t_{max} = 0.73\text{mm}$ $TC_{14} = 29.53\%$ $TC_{28} = 53.74\%$ $TC_{56} = 94.09\%$
					$A_0 = 5.82\text{mm}^2$ $t_m = 0.51\text{mm}$ $t_{max} = 0.63\text{mm}$ $TC_{14} = 28.18\%$ $TC_{28} = 36.43\%$ $TC_{56} = 82.99\%$
<i>BSair</i>					$A_0 = 2.91 \text{ mm}^2$ $t_m = 0.42\text{mm}$ $t_{max} = 0.87\text{mm}$ $TC_{14} = 48.11\%$ $TC_{28} = 71.48\%$ $TC_{56} = 67.35\%$
					$A_0 = 1.89 \text{ mm}^2$ $t_m = 0.29\text{mm}$ $t_{max} = 0.48\text{mm}$ $TC_{14} = 47.62\%$ $TC_{28} = 50.79\%$ $TC_{56} = 48.15\%$
					$A_0 = 2.32\text{mm}^2$ $t_m = 0.26\text{mm}$ $t_{max} = 0.49\text{mm}$ $TC_{14} = 50\%$ $TC_{28} = 89.66\%$ $TC_{56} = 91.81\%$

Table 6 (continued)

	7 DAYS (L ₀)	14 DAYS	28 DAYS	56 DAYS	SUMMARY
M-REF					$A_0 = 1.44 \text{ mm}^2$ $t_m = 0.19 \text{ mm}$ $t_{max} = 0.24 \text{ mm}$ $T_{C14} = 86.11\%$ $T_{C28} = 81.94\%$ $T_{C56} = 61.81\%$
					$A_0 = 1.2 \text{ mm}^2$ $t_m = 0.17 \text{ mm}$ $t_{max} = 0.17 \text{ mm}$ $T_{C14} = 59.17\%$ $T_{C28} = 79.17\%$ $T_{C56} = 71.67\%$
					$A_0 = 0.84 \text{ mm}^2$ $t_m = 0.10 \text{ mm}$ $t_{max} = 0.14 \text{ mm}$ $T_{C14} = 65.48\%$ $T_{C28} = 71.43\%$ $T_{C56} = 66.67\%$
M-REF _{air}					$A_0 = 4.33 \text{ mm}^2$ $t_m = 0.51 \text{ mm}$ $t_{max} = 1.17$ $T_{C14} = -14.90\%$ $T_{C28} = 37.88\%$ $T_{C56} = 48.50\%$
					$A_0 = 3.17 \text{ mm}^2$ $t_m = 0.38 \text{ mm}$ $t_{max} = 0.39 \text{ mm}$ $T_{C14} = 41.01\%$ $T_{C28} = 82.97\%$ $T_{C56} = 97.48\%$
					$A_0 = 4.10 \text{ mm}^2$ $t_m = 0.33 \text{ mm}$ $t_{max} = 0.39 \text{ mm}$ $T_{C14} = 60.73\%$ $T_{C28} = 91.46\%$ $T_{C56} = 94.88\%$

Analysis of 3 cracked areas from each group, where: A_0 : Initial crack area on the day of cracking; t_m : average crack thickness; t_{max} : the maximum thickness of each crack, Rh_x = Healing rate by age

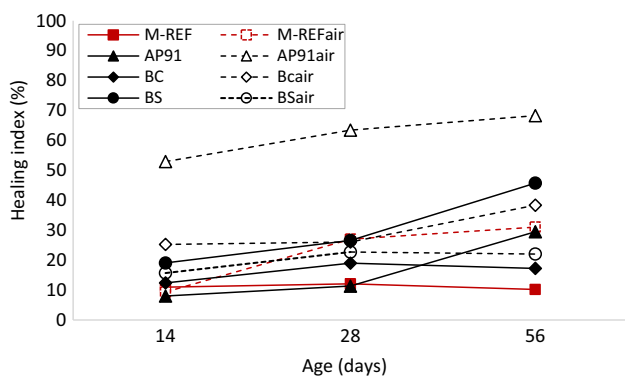


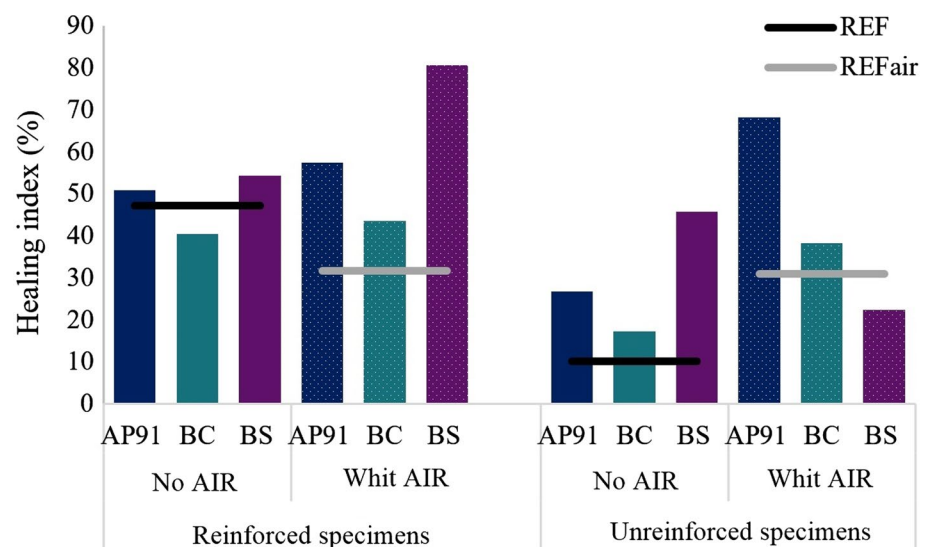
Fig. 6 Crack healing index over time for unreinforced specimens

others—also, the presence of reinforcement results in higher healing rates.

3.3 Scanning electron microscope and energy dispersive spectroscopy analysis

The visual analysis was performed in an optical stereomicroscope. The best healing index results were selected for microstructural analysis in SEM to verify the cement hydration and self-healing products. Thus, analysis for the group of reinforced specimens and the reference specimens without AIR was performed on the BS_{air} and AP91_{air}. For the first two, the analysis was performed on the cracked face (FIS)

Fig. 7 Comparison of the final healing index of reinforced (70 days) and unreinforced (56 days) specimens



and the fractured face (FRAT) to evaluate the precipitation difference between the cracked and conventional microstructure regions. Analysis of AP91air specimens was also performed for the group of specimens without reinforcement on the cracked and fractured faces.

The analysis results at 77 days in the reinforced specimens group are seen in Fig. 8 (specimens with FIS and FRAT faces) and 10 (specimens with FIS face).

All specimens showed crystal formation except for M-REF. The cracked faces of the BSair and AP91air specimens were composed of a cluster of precipitated crystals, while the cracked face of the reference specimen presented a smooth surface. As the substantial presence of crystals was observed only in the cracked faces (FIS), while the fractured faces (FRAT) showed a characteristic cementitious matrix, it was concluded that the crystals formation is related to bacterial activity and that even with the biological agents present in the cementitious matrix, due to the incorporation in the mixing water, the precipitation occurred in the crack region where water and oxygen are found.

The energy dispersive spectroscopy (EDS) analysis was performed to verify the composition of crystals precipitated in the cracks. The presence of Calcium, Oxygen, and Carbon atoms was verified, demonstrating CaCO_3 crystals formation. From the reference specimen analysis, peaks of the same compounds (C, Ca, and O) were observed, corroborating what was found in the visual analysis in Stereomicroscope—in which mortars without biological agents presented autogenous self-healing, precipitating calcium carbonate in lower amounts than specimens with biological agents (Fig. 9).

SEM microstructural analysis was also performed on the specimens without reinforcement that presented the best healing index, AP91air, both on the cracked and fractured faces. The images are presented in Fig. 10, which showed

a thick layer of precipitated crystals, where due to the C, Ca, and O peaks presence in the EDS, it is CaCO_3 possibly precipitated in larger quantities by the biological agents that, given the presence of AIR, had more space to metabolize and precipitate the product. From the reinforced specimens' images, a difference in the matrix between the cracked and the fractured faces was noticed, indicating that the bacteria developed substantially in the cracked region due to the greater space and greater water and oxygen presence.

3.4 Flexural tensile strength and compressive strength

The tests performed and discussed in this topic aimed to analyze the biological agents and AIR influence on cementitious materials' tensile and compressive strength properties. They were performed only on intact specimens without reinforcement at 28 and 56 days.

Figure 11 shows the flexural tensile strength results, where air incorporation impaired the flexural tensile performance of mortars, especially at 56 days, both in the reference specimens and the ones containing bacteria. Similar results were found by [30], who obtained an approximate 48% reduction in flexural strength in AIR-incorporated specimens compared to the reference specimens. In this study, the reduction at 56 days in the reference specimens was about 18%, while for the specimens with bacteria, the highest reduction was obtained in the BSair specimens (20%) and the lowest one in the AP9air specimens (8%).

It was also noted that the AP91air and BCair specimens presented tensile strength values higher than the reference AIR-incorporated specimens, but not those without AIR. At 56 days, the specimens without AIR did not reach results higher than the reference one; however, the BS and BC specimens obtained similar results.

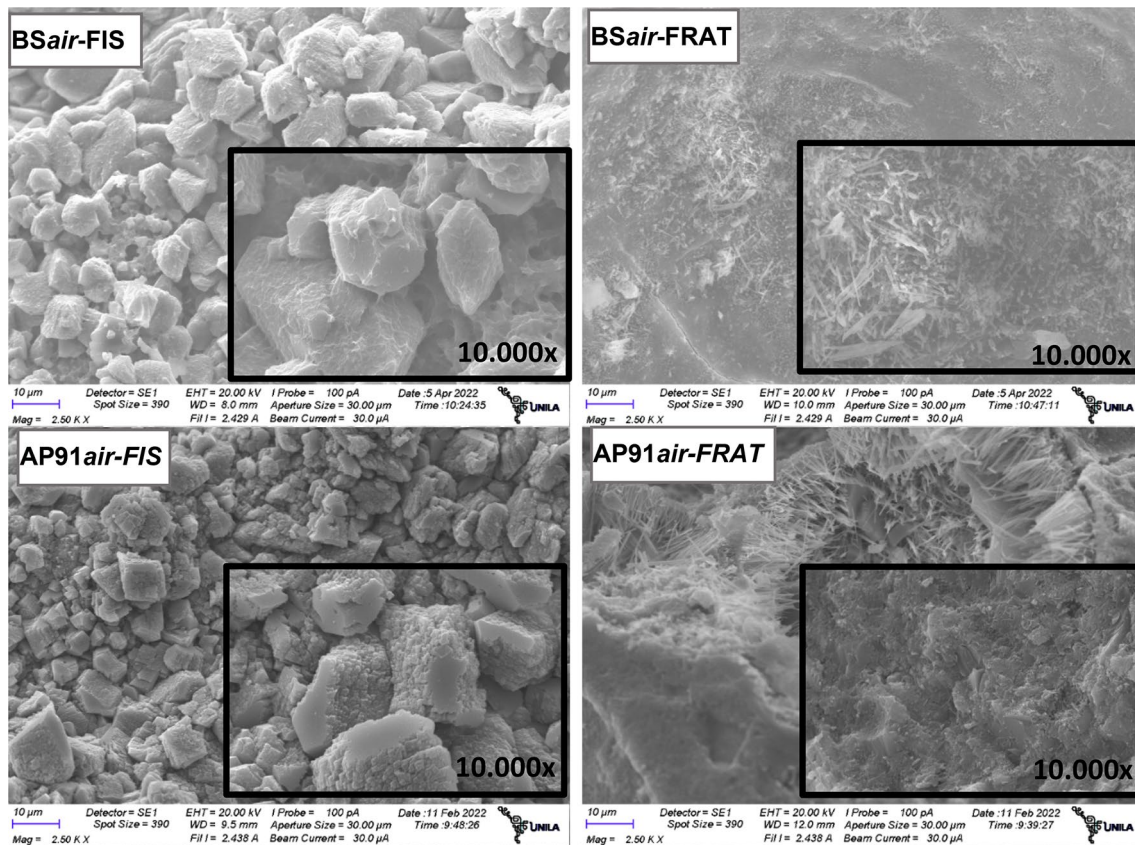


Fig. 8 SEM microstructural images of reinforced specimens with a higher healing index at 2500 \times and 10,000 \times magnification in the crack region (FIS) and fractured face (FRAT)

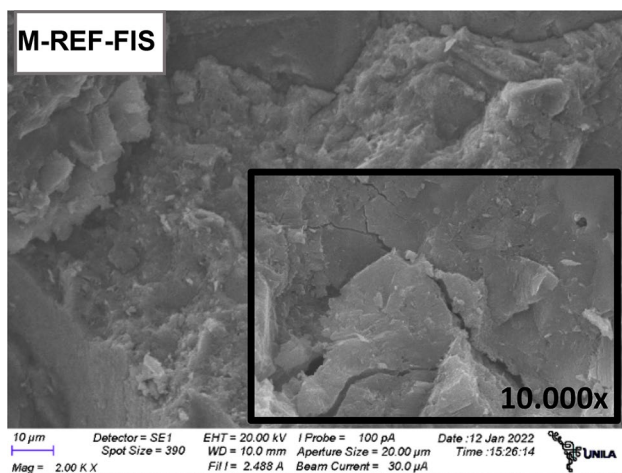


Fig. 9 SEM microstructural images of the cracked region (FIS) of the reference specimens at 2500 \times and 10,000 \times magnification

Figure 12 shows the specimens' compressive strength values, where all specimens, except for the variations M-REF, M-REFair, BS, and BSair, decreased strength at 56 days compared to those at 28 days [17]. Reported a similar result,

where 4 out of 6 variations containing bacterial solution immobilized in expanded pearlite presented strength values at 84 days lower than those at 28 days. It was assumed that, in this study, the reduction occurred due to the saline solution influence used for biological agent dilution, which is harmful to the cement matrix over time. In this context, it is suggested that future studies use different solutions to dilute bacteria to attenuate or eliminate the decrease in compressive strength obtained in this work. It may also have been influenced by the calcium-based product leaching processes [19].

A decrease in the compressive strength of the AIR-incorporated specimens was observed, similar to the tensile strength results [30]. Reported a 56% reduction in the specimens' compressive strength at 28 days. The authors cited that this decrease was caused by the additional air voids in the matrix originating with AIR. In this study, BCair and AP91air bacteria specimens reduced the compressive strength by 21.64% and 5.5%, respectively, while BSair showed a slight increase of 1.17%, all with respect to M-REFair.

Ultimately, determining the efficiency of CaCO₃ precipitating biological agent insertion for autonomous self-healing

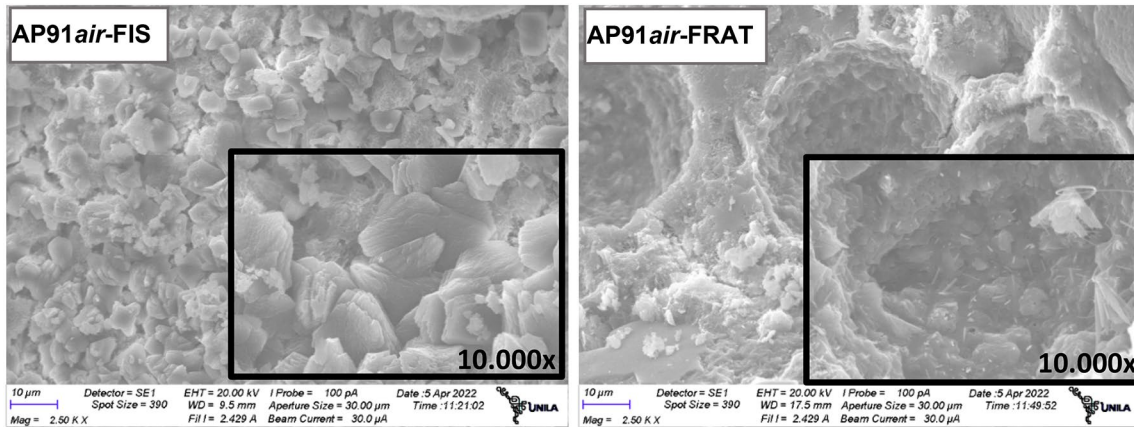


Fig. 10 SEM microstructural image of the unreinforced specimens with the highest healing index in the region of the crack (FIS) and fractured face (FRAT) at 2500× and 10,000× magnification

Fig. 11 Flexural tensile strength of intact specimens with AP91, BC, and BS bacteria at 28 and 56 days

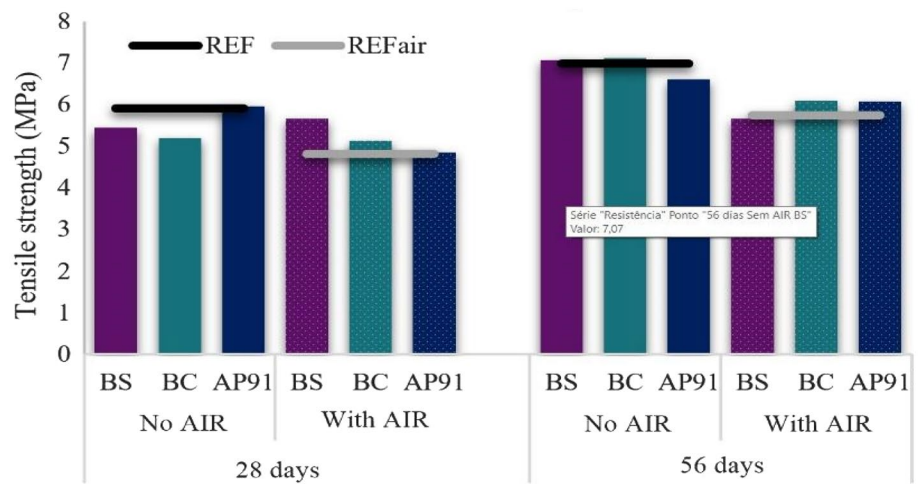
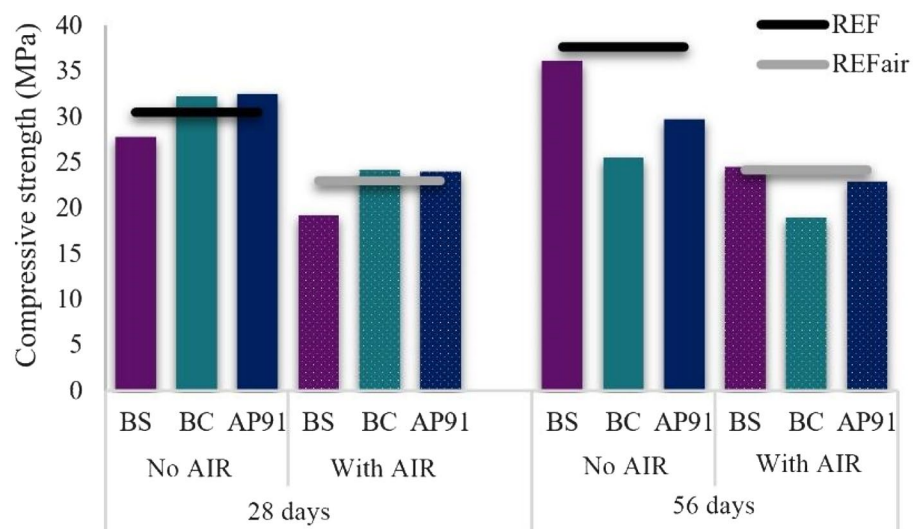


Fig. 12 Compressive strength of intact specimens with AP91, BC, and BS bacteria at 28 and 56 days



of cracks in cementitious materials should follow a meticulous methodology, performing visual evaluations of cracks, durability analysis, and recovery of mechanical properties, establishing a correlation between them.

Notably, using these microorganisms can corroborate to guarantee concrete structures' service life and durability. The increase in service life reduces the demand for natural resources to build new structures, preserving resources and minimizing waste generation [32], contributing to the sustainability of the built environment.

4 Conclusions

In this study, it was found that the incorporation of the genera *Bacillus subtilis* (AP91), *Bacillus cf. subtilis* (BS), and *Bacillus cf. cereus* (BC) bacteria promote self-healing of cracks in cement-based matrices by metabolic precipitation of calcium carbonate. The *Bacillus cf. subtilis*, isolated from a building in Foz do Iguacu-PR, Brazil, presented the best performance, recovering cracks with a thickness of 1.58 mm in air-incorporated matrices.

The difference in bacteria performance was observed in the self-healing of cracks for specimens with and without reinforcement, with more favorable healing indexes on reinforced specimens.

The most promising self-healing results were verified in air-incorporated matrices; however, air incorporation in the matrix tends to reduce the mechanical properties of the composite. The SEM analysis of the cracked region of the fractured face (interior of the specimen) showed that despite being dispersed in the matrix, bacteria tend to metabolize and precipitate carbonates in the cracked and pore regions, where there is more oxygen and water.

Adding CaCO₃ precipitating biological agent to the cement matrix is promising for cracks self-healing since the viability of bacteria is increased in air-incorporated matrices. Using microorganisms increases the durability of cementitious materials as the diameter of pores and thickness of cracks decreases over time, minimizing the need for repairs and improving the building's service life. However, further studies are needed to improve the laboratory procedures of concrete self-healing by biological agents, develop biomaterials for application in actual constructions, increase durability, reduce recovery costs, and extend concrete structures' service life.

Acknowledgements To Araucária Foundation and PRPPG for funding the research and to the Performance, Structures, and Materials Laboratory (LADEMA) and Environmental Biotechnology Laboratory for research support.

Author contributions SKL: experimental work and data collection, Discussion of results, writing-original draft preparation. EP: funding

acquisition; Conceptualization, Supervision, Methodology, writing reviewing, and editing. MRZP: supervision, methodology, discussion of results, supervision, writing reviewing, and editing. PG: collection and isolation of bacterial strains.

Funding Universidade Federal da Integração Latino Americana and, Fundação Araucária [Convênio P&DI N° 104/2022 PDI].

Data availability The data will be made available upon request to the authors.

Declarations

Conflict of interest The authors declare that there is no conflict of interest.

References

1. Felix EF, Balabuch TJR, Posterli MC, Possan E, Carrazedo R (2018) Service life analysis of reinforced concrete structure under uniform corrosion through ANN model coupled to the FEM. *Revista ALCONPAT* 8(1):1–15. <https://doi.org/10.21041/ra.v8i1.256>
2. Jonkers D (2011) Wise crack. *Engineer* 11-APRIL:28–29
3. Van Tittelboom K, De Belie N (2013) Self-healing in cementitious materials—a review. *Materials* 6:2182–2217. <https://doi.org/10.3390/ma6062182>
4. Cappellesso VG, Van Mullem T, Gruyaert E, Van Tittelboom K, De Belie N (2023) Bacteria-based self-healing concrete exposed to frost salt scaling. *Cement Concr Compos* 105016. <https://doi.org/10.1016/j.cemconcomp.2023.105016>
5. Jonkers HM (2011) Bacteria-based self-healing concrete. *Heron* 56:1–12
6. Schwantes-Cezario N, Nogueira GSF, Toralles BM (2017) Biocimentação de compósitos cimentícios mediante adição de esporos de *Bacillus subtilis* AP91. *Revista de Engenharia Civil IMED* 4:142–158. <https://doi.org/10.18256/2358-6508.2017.v4i2.2072>
7. Wiktor V, Jonkers HM (2011) Un nouveau béton auto-cicatrisant grâce à l'incorporation de bactéries. *Matériaux Tech* 99:565–571. <https://doi.org/10.1051/mattech/2011110>
8. De Rooij M, Van Tittelboom K, de Belie N, Schlangen E (2013) RILEM TC 221-SHC: self-healing phenomena in cement-based materials. Springer, Netherlands
9. Jonkers HM, Thijssen A, Muyzer G et al (2010) Application of bacteria as self-healing agent for the development of sustainable concrete. *Ecol Eng* 36:230–235. <https://doi.org/10.1016/j.ecoleng.2008.12.036>
10. De Belie N, De Muynck W (2009) Crack repair in concrete using biodeposition. *Concrete Repair, Rehabilitation and Retrofitting II—Proceedings of the 2nd International Conference on Concrete Repair, Rehabilitation and Retrofitting, ICCRRR* 2:291–292. <https://doi.org/10.1201/9781439828403.ch107>
11. Van TK, De BN, De MW, Verstraete W (2010) Cement and concrete research use of bacteria to repair cracks in concrete. *Cem Concr Res* 40:157–166. <https://doi.org/10.1016/j.cemconres.2009.08.025>
12. Jonkers HM, Thijssen A (2010) Bacteria Mediated of Concrete Structures. 2nd International Symposium on Service Life Design for Infrastructure 4–6 October 2010, Delft, The Netherlands 833–840
13. Ghellere P (2021) Seleção e avaliação de bactérias produtoras de CaCO₃ na recuperação de fissuras dos materiais a base de

- cimento. (Dissertação) Programa de Pós-Graduação em Engenharia Civil. Universidade Federal da Integração Latino Americana, pp 1–115. <https://dspace.unila.edu.br/handle/123456789/6446>
14. Schwantes-Cezario N, Peres MVNDN, Fruet TK et al (2018) Crack filling in concrete by addition of bacillus subtilis spores—preliminary study. *DYNA (Colombia)* 85:132–139. <https://doi.org/10.15446/dyna.v85n205.68591>
 15. Ramachandran SK, Ramakrishnan V, Bang SS (2001) Remediation of concrete using micro-organisms. *ACI Mater J* 98(1):3–9. <https://doi.org/10.14359/10154>
 16. Luo M, Qian CXC-X, Li RYR-Y (2015) Factors affecting crack repairing capacity of bacteria-based self-healing concrete. *Constr Build Mater* 87:1–7. <https://doi.org/10.1016/j.conbuildmat.2015.03.117>
 17. Pacheco F (2020) Análise da eficácia dos mecanismos de autorregeneração e autocicatrização do concreto. (Tese) Programa de Pós-Graduação em Engenharia Civil. Universidade do Vale do Rio dos Sinos UNISINOS, São Leopoldo. <http://www.repositorio.jesuita.org.br/handle/UNISINOS/9376>
 18. Wiktor V, Jonkers HMMHM (2011) Cement & concrete composites quantification of crack-healing in novel bacteria-based self-healing concrete. *Cement Concr Compos* 33:763–770. <https://doi.org/10.1016/j.cemconcomp.2011.03.012>
 19. Cappellesso VG (2018) Avaliação da autocicatrização de fissuras em concretos com diferentes cimentos. Dissertação de Mestrado. Universidade Federal Do Rio Grande Do Sul Escola de Engenharia Programa de Pós-Graduação em Engenharia Civil: Construção e Infraestrutura
 20. Associação Brasileira de Normas Técnicas (2005) NBR 13279 Argamassa para assentamento e revestimento de paredes e tetos - Determinação da resistência à tração na flexão e à compressão. Associação Brasileira de Normas Técnicas, pp 1–9
 21. Sahmaran M, Yildirim G, Erdem T K (2013) Self-healing capability of cementitious composites incorporating different supplementary cementitious materials. *Cement Concr Compos* 35(1):89–101. <https://doi.org/10.1016/j.cemconcomp.2012.08.013>
 22. Gagné R, Argouges M (2012) A study of the natural self-healing of mortars using air-flow measurements. *Mater Struct/Materiaux et Constr* 45:1625–1638. <https://doi.org/10.1617/s11527-012-9861-y>
 23. Xu H, Lian J, Gao M et al (2019) Self-healing concrete using rubber particles to immobilize bacterial spores. *Materials*. <https://doi.org/10.3390/ma12142313>
 24. Sidiq A, Gravina R, Giustozzi F (2019) Is concrete healing really efficient? A review. *Constr Build Mater* 205:257–273. <https://doi.org/10.1016/j.conbuildmat.2019.02.002>
 25. Ferrara L, Asensio EC, Monte FL et al (2018) Experimental characterization of the self-healing capacity of cement based materials: an overview. *Proceeding*. <https://doi.org/10.3390/icem18-05322>
 26. Hilloulin B, Legland JB, Lys E et al (2016) Monitoring of autogenous crack healing in cementitious materials by the nonlinear modulation of ultrasonic coda waves, 3D microscopy and X-ray microtomography. *Constr Build Mater* 123:143–152. <https://doi.org/10.1016/j.conbuildmat.2016.06.138>
 27. Roig-Flores M, Pirritano F, Serna P, Ferrara L (2016) Effect of crystalline admixtures on the self-healing capability of early-age concrete studied by means of permeability and crack closing tests. *Constr Build Mater* 114:447–457. <https://doi.org/10.1016/j.conbuildmat.2016.03.196>
 28. Schwantes N (2017) Desempenho de Bacillus sp. na biocimentação de materiais cimentícios (Dissertação). Programa de Pós-Graduação em Edificações e Saneamento. Universidade Estadual de Londrina. <http://www.bibliotecadigital.uel.br/document/?code=vtls000211479>
 29. Chen B, Sun W, Sun X et al (2021) Crack sealing evaluation of self-healing mortar with Sporosarcina pasteurii: influence of bacterial concentration and air-entraining agent. *Process Biochem* 107:100–111. <https://doi.org/10.1016/j.procbio.2021.05.001>
 30. Justo-Reinoso I, Reeksting BJ, Hamley-Bennett C et al (2022) Air-entraining admixtures as a protection method for bacterial spores in self-healing cementitious composites: healing evaluation of early and later-age cracks. *Constr Build Mater* 327:126877. <https://doi.org/10.1016/j.conbuildmat.2022.126877>
 31. Hollmann CF (2020) Avaliação da influência de aditivos cristalizantes na resistência à penetração de íons cloreto em concretos fissurados (Dissertação) Programa de Pós-Graduação em Engenharia Civil: construção e infraestrutura. Universidade Federal do Rio Grande do Sul, Rio Grande do Sul
 32. Possan E, Molin DCCD, Andrade JJO (2018) A conceptual framework for service life prediction of reinforced concrete structures. *J Build Pathol Rehabil*. <https://doi.org/10.1007/s41024-018-0031-7>

Publisher's Note Springer Nature remains neutral with regard to jurisdictional claims in published maps and institutional affiliations.

Springer Nature or its licensor (e.g. a society or other partner) holds exclusive rights to this article under a publishing agreement with the author(s) or other rightsholder(s); author self-archiving of the accepted manuscript version of this article is solely governed by the terms of such publishing agreement and applicable law.